



3C protease-independent production of foot-and-mouth disease virus-like particles in *Pichia pastoris*

Zhiyao Li¹ · Hu Dong¹ · Shuanghui Yin¹ · Manyuan Bai¹ · Yun Zhang¹ · Yaozhong Ding¹ · Shiqi Sun¹ · Huichen Guo^{1,2}

Received: 4 January 2025 / Revised: 25 April 2025 / Accepted: 1 May 2025
© The Author(s) 2025

Abstract

The inactivated vaccines have played a pivotal role in the control and eradication of foot-and-mouth disease (FMD). However, certain safety concerns remain. Recently, virus-like particles (VLPs) have gradually become a research hotspot. As the eukaryotic expression system with the lowest production costs, the production of VLPs using *Pichia pastoris* has significant potential. During the natural infection process of FMD virus (FMDV), the polyprotein P1 is cleaved by 3C protease to form VP0, VP3, and VP1, which are subsequently assembled into VLPs. In this study, we adopted an alternative approach, co-expressing VP0, VP3, and VP1 without 3C protease for the production of FMDV VLPs in *P. pastoris*. The western blot (WB) assays showed variable protein expression on the same plasmid. VP0 was the highest, while VP3 and VP1 were similar. Furthermore, the order of proteins on the plasmid also mattered. The results indicated that His₆ tags at VP0, VP3, and VP1 N-termini significantly affected VLPs assembly. The three-dimensional structure of FMDV revealed that the N-terminus of VP3 and VP1, which are situated in the external space of VLPs, can be fused with His₆ tag. Inserting His₆ tags into the G-H loop region of VP1 did not hinder assembly, thus providing a reference for the affinity purification of capsid and VLPs assembly. Here, FMDV VLPs were successfully produced independently of 3C protease, avoiding the uncontrollable cleavage efficiency and toxicity of 3C protease in host cells and demonstrating the potential of *P. pastoris* for FMDV VLPs production.

Key points

- FMDV VLPs could be produced in *P. pastoris* by a 3 C protease-independent approach
- Optimal expression of FMDV VLPs in *P. pastoris* is achieved at pH 7 with 72-h induction
- His₆ can be fused to the G-H region and C-terminus of VP1 and C-terminus of VP3 without affecting the VLPs assembly

Keywords Foot-and-mouth disease · Virus-like-particles · 3C protease · Purification · *Pichia pastoris*

✉ Huichen Guo
guohuichen@caas.cn

Zhiyao Li
2021207044@stu.njau.edu.cn

Hu Dong
donghu@caas.cn

Shuanghui Yin
yinshuanghui@caas.cn

Manyuan Bai
baimanyuan@caas.cn

Yun Zhang
zhangyun@caas.cn

Yaozhong Ding
dingyaozhong@caas.cn

Shiqi Sun
sunshiqi@caas.cn

¹ State Key Laboratory for Animal Disease Control and Prevention, College of Veterinary Medicine, Lanzhou University, Lanzhou Veterinary Research Institute, Chinese Academy of Agricultural Sciences, Lanzhou 730000, China

² Gansu Province Research Center for Basic Disciplines of Pathogen Biology, Lanzhou 730046, China

Introduction

Foot-and-mouth disease (FMD) is a highly contagious and virulent infectious disease that mainly affects cloven-hoofed animals such as pigs, cattle, and sheep (Alexandersen et al. 2003). Once infected, animals show symptoms of fever and blisters appear on the mouth, nose, tongue, hooves, or udder. These blisters then rupture and form scabs (Arzt et al. 2011). Infection with FMD leads to a significant reduction in the animal production capacity, which has a negative impact on local livestock production and economic development. Although FMD has now been eradicated in some developed countries, it still persists in Asia, Europe, Africa, and South America (Subramaniam et al. 2013). The injection of inactivated FMD vaccines is currently the most effective method of controlling FMD. However, several challenges remain in the production process of inactivated FMD vaccines, including the need for expensive biosafety facilities and the potential risk of virus leakage (Robinson et al. 2016). Therefore, the development of a safe and highly effective FMD vaccine is of particular importance.

FMD virus (FMDV) belongs to the *Picornaviridae* family and the genus *Aphthovirus*. It is a single-stranded positive-sense RNA virus without an envelope. The diameter of the virion is approximately 30 nm, and the genome size is 8500 nts, encoding a structural protein P1 and non-structural proteins P2 and P3. The precursor P1 is cleaved by 3C protease to generate VP0, VP3, and VP1 proteins. VP0 is cleaved into VP2 and VP4 during virion assembly. Sixty copies of VP1–VP4 proteins are assembled into VLPs and VP4 is located inside (Acharya et al. 1989). Virus-like particles (VLPs) can mimic the morphological structure of viruses but do not contain nucleic acid, making them a very safe and ideal vaccine type (Chackerian 2007; Migniqui et al. 2019). Currently, FMDV VLPs have been successfully produced in mammalian cells (Migniqui et al. 2020; Polacek et al. 2013), insect cells (Vivek Srinivas et al. 2016), and plant cells (Veerapen et al. 2018). During the processing of viral polypeptide, the 2A peptide of picornaviruses cleaves the 2A-2B protein through a ribosome-skipping mechanism. Expression of P1-2A-3C has usually been used to produce VLPs in mammalian cells or insect cells. However, due to the non-specific cleavage of 3C, it can not only cleave P1 but also cleave the host protein, resulting in transcriptional termination and even host cell death (Belsham et al. 2000; Capozzo et al. 2002; Migniqui et al. 2013). Although FMDV 2A (F2A) protein does not exhibit cytotoxicity like 2A of poliovirus (PV) or human rhinovirus (HRV), the cleavage efficiency of F2A is the lowest in eukaryotic cells compared to that of those assigned virus 2A, equine rhinitis

A virus 2A, and porcine teschovirus-1 2A (de Felipe et al. 2006; Kim et al. 2011). As the lowest cost eukaryotic expression system, *Pichia pastoris* is widely used in preparing VLP vaccines, such as hepatitis B vaccine and human papillomavirus vaccine which are licensed for production using *P. pastoris* (McAleer et al. 1984; Sasagawa et al. 1995; Smith et al. 2011). However, several studies have attempted to obtain VLPs of picornaviruses using *P. pastoris*, such as enterovirus 71 (Zhang et al. 2015), coxsackievirus A16 (Feng et al. 2016), and PV (Sherry et al. 2020). Unfortunately, there has been no research on the production of FMDV VLPs in *P. pastoris* so far. Our previous research has shown that the effect of 3C protease on *P. pastoris* is different. The cleavage activity of 3C is strongly affected in acidic environment. Regardless of the toxicity problem of 3C in mammalian cells or the cleavage efficiency problem in *P. pastoris*, they severely limit the production and promotion of FMDV VLPs. Therefore, exploring 3C protease-independent production of FMDV VLPs is well worthy of in-depth research (de Felipe et al. 2006; Kim et al. 2011).

Here, we investigated the possibility of producing FMDV VLPs by directly expressing the capsid proteins VP0, VP3, and VP1 in *P. pastoris*, avoiding the use of 3C protease. After expressing these subunit proteins VP0, VP3, and VP1, we found that the expression levels of these three proteins varied in yeast. The expression levels of the three proteins were optimized by adjusting the position of their expression cassettes on the plasmid. Considering the acid resistance characteristic of FMDV VLPs, the optimal pH and induction time of the strain were tested. The protein expression level was highest when induced at pH 7 for 72 h. To facilitate the purification of the VLPs, the tertiary structure analysis of the VLP revealed that the G-H loop region and C-terminus of VP1 and the C-terminus of VP3 could be fused with His₆ tags without affecting the VLPs assembly. This study provides a new technical strategy and research basis for the production of FMDV VLPs using *P. pastoris*.

Materials and methods

Strains, plasmids, and reagents

The genes of VP0 with the VP2 (H2145Y) mutation, VP3, VP1 with the mutation (N1017D), VP1-GHH, VP3-CH, and VP1-CH (see Supplementary Material for sequences) were synthesized and inserted into pPink-HC by Nanjing GenScript (Nanjing, China) and stored in our laboratory. Anti-FMDV O type polyclonal antibodies were preserved at Lanzhou Veterinary Research Institute. The pPink-HC plasmid and *PichiaPink*TM Strain 1 (*P. pastoris*) were purchased

from Invitrogen (Grand Island, NY, USA) while anti-His₆ antibodies were obtained from Solarbio (Beijing, China).

Plasmid construction and transformation

The DNA sequences of the N-termini of VP0, VP3, and VP1 genes were fused with the sequences for a His₆ tag. An enterokinase recognition site (DDDDK) inserted between the tag and the target protein. For VP1-GHH protein, His₆ comprising (GGGGS)₂ at its N- and C-termini was inserted at residue 136 of VP1 protein. VP3-CH and VP1-CH proteins had a His₆-(GGGGS)₂ sequence added at their C-termini. These respective genes encoding these proteins were all synthesized and inserted into the pPink-HC. Next, the VP3 and VP0 expression cassettes were digested by *Bgl*II/*Bam*HI and then inserted into pPink-VP1 plasmid. The pPink-VP1/VP3/VP0 (pPink-130) plasmid, the pPink-VP1-GHH/VP3/VP0 (GHH) plasmid, the pPink-VP1/VP3-CH/VP0 (3 CH) plasmid, and the pPink-VP1-CH/VP3/VP0 (1 CH) plasmid were generated using the same procedure. The plasmids were linearized by *Spe*I for electroporation into *P. pastoris*. Yeast transformation and selection of positive colonies were performed as previously (Zhang et al. 2015).

SDS-PAGE and western blot analysis

SDS-PAGE and western blot were performed according to the previous description (Li et al. 2024; Xie et al. 2019). In brief, the expressed proteins were separated on 12% polyacrylamide gels and stained with Coomassie blue R250. For western blot, the gels were transferred to nitrocellulose membranes using a wet transfer method after SDS-PAGE. Then, the membranes were blocked with 5% skimmed milk and probed with a mouse-derived His₆ antibody (diluted 1:1000) or an anti-FMDV polyclonal antibody (diluted 1:1000) followed by a horseradish peroxidase (HRP)-conjugated second antibody (Solarbio, Beijing, China). Finally, the 3,3',5,5'-tetramethylbenzidine (TMB) kit (Beyotime, Shanghai, China) was used for color development.

Purification of FMDV VLPs

The positive yeast strains were inoculated into 30 mL of BMGY medium (1% yeast extract, 2% peptone, 100 mM potassium phosphate (pH 6.0), 1.34% yeast nitrogen broth, 0.4 mg/L biotin, 1% glycerol), and cultivated at 30 °C until the OD_{600 nm} reached 2. Then, the samples were centrifuged to collect the yeast pellet. The medium was replaced with BMMY (1% yeast extract, 2% peptone, 100 mM potassium phosphate (pH 6.0), 1.34% yeast nitrogen broth, 0.4 mg/L biotin, 1% methanol) and the pellet was resuspended to make the OD_{600 nm} reach 1 for induction. Methanol was added every 24 h to a final concentration of 0.75%, and the cells

were cultured in a shaking incubator at 30 °C with a speed of 200 rpm for 72 h. After induction, the cell pellet was disrupted by sonication at 350 W for 20 min. The supernatant was centrifuged at 12,000 rpm for 30 min and dialyzed overnight (300 mM NaCl, 10 mM Tris, 50 mM KCl, 2 mM MgCl₂, 1% Triton X-100, and 0.1 mM phenylmethylsulphonyl fluoride (PMSF), pH 8.0).

For sucrose gradient purification, the sample was first dialyzed. Then, it was centrifuged at 12,000 rpm for 30 min. Next, 1 mL sample was added to the top of the 15–50% (w/v) sucrose gradient solution and centrifuged at 35,000 rpm for 3 h. Then, the samples were separated and collected in 500 µL per tube from the top to the bottom of the gradient. The absorbance of each fraction was measured using a UV spectrophotometer. Fractions with the highest absorbance were selected for further analysis.

For affinity chromatography, the supernatant was subjected to affinity chromatography after dialysis and then washed with 10 mM imidazole buffer. The target proteins were then eluted with 300 mM imidazole buffer. For urea treatment, the same procedure was followed, but with an 8 M urea imidazole buffer. After ultrafiltration and concentration with phosphate-buffered saline (PBS), the VLPs were collected and detected.

Particle size detection and electron microscopy observation

One milliliter of purified samples was taken and their hydrodynamic particle size was measured by a dynamic light scatterer (DLS) instrument (Malvern, Worcestershire, UK) to evaluate the assembly efficiency. VLP samples were added to 200-mesh copper grids and negatively stained with 3% phosphotungstic acid. Finally, the samples were observed by transmission electron microscopy (TEM) using a Hitachi (Tokyo, Japan) H-7100 FA microscope (operating at 80 kV with a field emission gun).

Quantification of FMDV VLPs by enzyme-linked immunosorbent assay (ELISA)

The quantification of VLPs was performed as previously described (Dong et al. 2022). In brief, 96-well plates were coated overnight with 0.5 µg trapping antibody M170 (100 µL per well) diluted with carbonate buffer (pH 9.6) at 4 °C. The next day, the plates were blocked with 1% bovine serum albumin (BSA) at 37 °C for 1 h. Serially diluted antigen samples were then added to the plates and incubated at 37 °C for 1 h, followed by the guinea pig anti-FMDV antibodies and the horseradish peroxidase (HRP)-conjugated rabbit anti-guinea pig IgG and incubated at 37 °C for 30 min. Finally, TMB was added for color development for 15 min before termination with 2 M H₂SO₄ and the OD_{450 nm} value

was measured. According to the standard curve generated based on the known FMDV virion concentration, the relative antigen content in the sample was determined, and the concentration of VLPs was then calculated.

Data analysis

Data presented in the paper, and one-way analysis of variance were performed using GraphPad Prism 8 (Dotmatics, Boston, USA). Statistically significant differences are indicated in figures by asterisk (“*” for $0.01 \leq P < 0.05$, “**” for $P < 0.01$).

Results

3C protease-independent production of FMDV structural proteins in *P. pastoris*

To reduce the uncontrollable cleavage effect of 3C protease, a 3C protease-independent strategy was used to produce FMDV VLPs in *P. pastoris* and a series of plasmids were constructed (Fig. 1a and d). To verify whether the structural proteins of FMDV could be successfully expressed in the yeast *P. pastoris*, the cell lysate supernatant of pPink-031 and pPink-130 was analyzed by western blot (WB) after

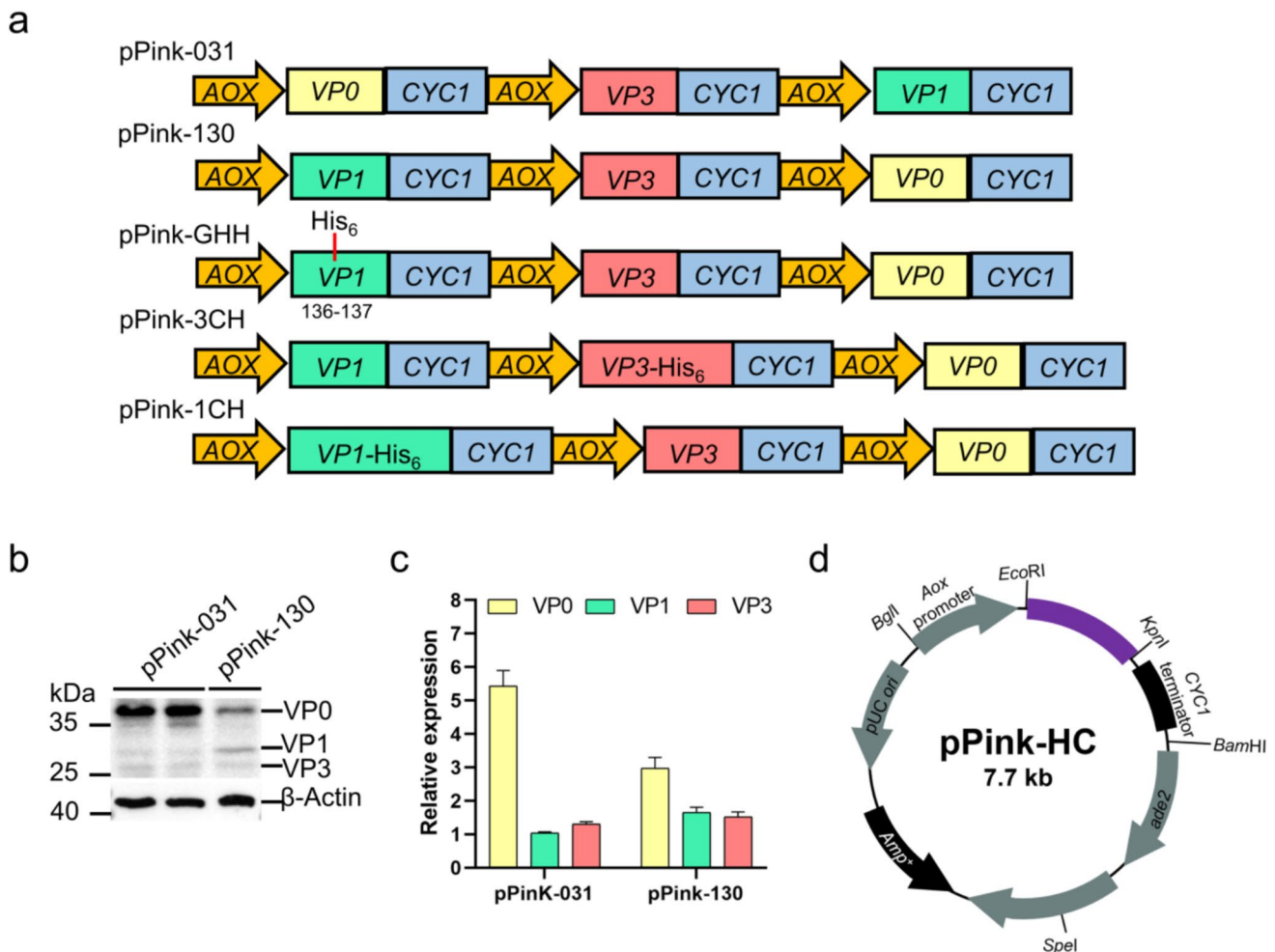


Fig. 1 Comparison of the expression of structural proteins of different plasmids (pPink-031 and pPink-130). **a** Schematic diagram of the engineered plasmids in this study. VP0, VP3, and VP1 proteins are expressed under the control of three alcohol oxidase (AOX) promoters. The gene expression cassettes are placed in the order VP0-VP3-VP1 on the pPink-HC plasmid to generate pPink-031 plasmid. The VP0 and VP3 genes cassettes were switched to generate pPink-130 plasmid, and on the basis of pPink-130 plasmid, the amino acid sequence for (GGGGS)₂-His₆-(GGGGS)₂ was inserted at residue 136

of VP1 amino acid sequence to generate pPink-GHH plasmid; the sequence for His₆ was fused to the sequence for the C-terminus of VP3 or VP1 to generate pPink-3 CH plasmid and pPink-1 CH plasmid. WB detection (**b**) and quantification (**c**) of the structural proteins of pPink-031 plasmid and pPink-130 plasmid. **d** The map of the pPink-HC vector, showing the AOX promoter, the CYC1 terminator, the *ade* (encoding phosphoribosylaminoimidazole carboxylase, used as the selection marker) and the *Amp*^r marker, and the origin of replication

induction. The results showed that three specific bands corresponding to VP3 (25 kDa), VP1 (27 kDa), and VP0 (37 kDa) were detected for pPink-031 by WB, but the expression levels of the three proteins were not equal. VP0 was the highest, about six times higher than the other two proteins. VP3 was the next highest and VP1 was the lowest. Subsequently, by exchanging the positions of the VP0 and VP1 expression cassettes on the pPink-031 plasmid, the expression levels of VP0 and VP1 were optimized and the difference between VP0 and VP1/VP3 was diminished (Fig. 1b and c). These results indicate that the expression of FMDV structural proteins in *P. pastoris* varies, and the difference in the expression levels of the three proteins was reduced by switching the order of their expression cassettes on the plasmid.

Purification and identification of FMDV VLPs

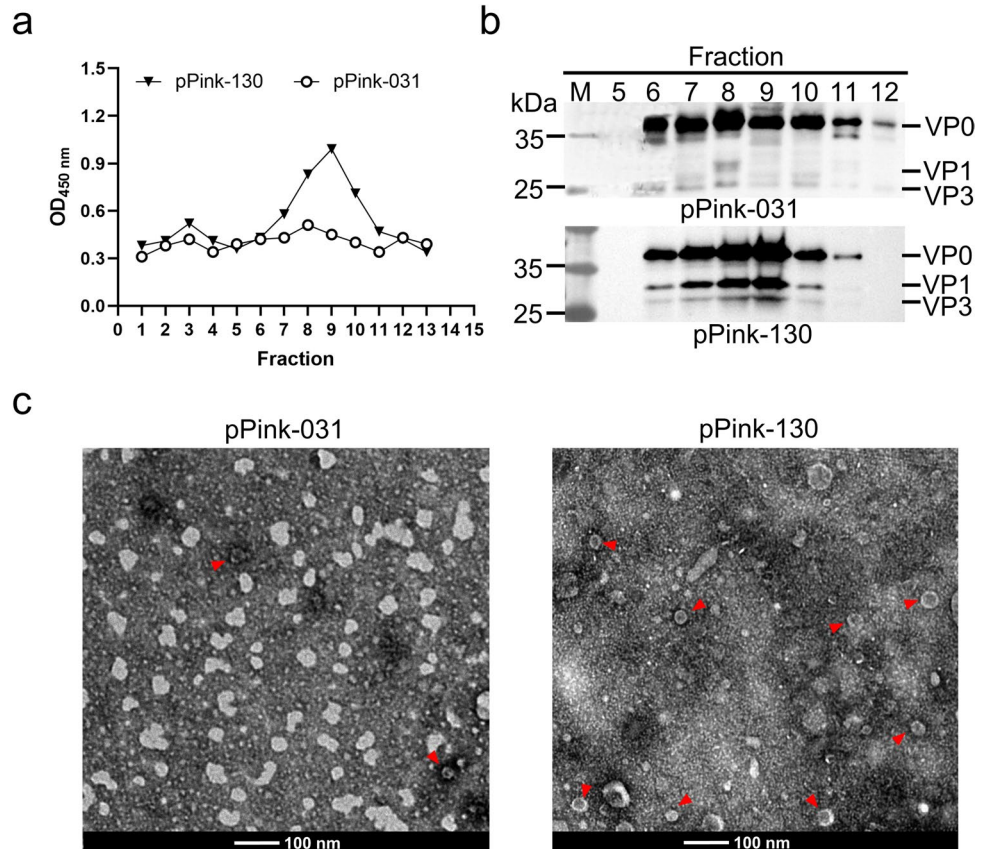
To assess whether these structural proteins could be correctly assembled into VLPs, the lysate was dialyzed and then purified by sucrose gradient sedimentation. One milliliter of supernatant was added to a 15–50% (w/v) sucrose gradient and then centrifuged at 35,000 rpm for 3 h. The fractions were then collected from top to bottom of the gradient in tubes containing 500 μ L each, and the purified VLPs were

detected by ELISA. The results showed that fraction 8 of pPink-031 had the highest absorbance value at 450 nm. However, fraction 9 of pPink-130 had the highest absorbance value, which was higher than that of pPink-031, indicating the presence of correctly assembled VLPs (Fig. 2a). Fractions 5–12 were subjected to WB detection and the structural proteins VP0, VP3, and VP1 were co-sedimented, indicating that the VLPs were composed of these three subunits (Fig. 2b). The purified samples of pPink-031 and pPink-130 were then examined by TEM and regular particles with a diameter of approximately 30 nm were observed (Fig. 2c). These results show that after purification, pPink-130 had a higher yield of VLPs than pPink-031. Only when the three structural proteins were expressed as uniformly as possible, the assembly of VLPs was facilitated.

Optimization of expression conditions for pPink-130

To optimize the expression of pPink-130, a screening of its culture conditions was performed. First, the strain was inoculated into buffered glycerol-complex medium for yeast (BMGY) and cultured until the OD_{600 nm} reached the range of 2 to 6. Cells were then harvested and resuspended in buffered methanol complex medium for yeast (BMMY) at pH 5 to 8 to adjust the initial OD_{600 nm} to 2. At 12-h intervals,

Fig. 2 Purification and TEM of pPink-031 and pPink-130 VLPs. Analysis of the thirteen sucrose gradient fractions by ELISA (a) and WB (b). c TEM observation of the purified VLPs. VLPs are marked with red triangles. Scale bar shows 100 nm



200 μ L aliquots of the culture broth were sampled to measure OD_{600 nm} and at the same time, 100 μ L of the culture was collected and pelleted. An equal volume of acid-washed glass beads (0.5 μ m) was added, followed by vortexing to disrupt the cells. The supernatant was then collected by centrifugation at 12,000 rpm for 10 min for WB analysis. By measuring OD_{600 nm} and protein expression at different time points, it was observed that strain growth and protein expression showed a positive correlation with time. After 72 h, the strain OD_{600 nm} did not increase. The OD_{600 nm} showed minimal variation at pH 5 and 6. However, at pH 7, the OD_{600 nm} value dropped from 11 to 9. Growth of the strain was severely inhibited, resulting in cell death at pH 8 (Fig. 3a and b). The WB results showed that the protein expression level increased with time within a specific time period. Moreover, it was worth noting that the target proteins were barely detectable at pH 8, while the peak was reached after 72 h of induction under other suitable pH conditions (Fig. 3c–e). Overall, pPink-130 achieved the most favorable expression level at pH ≤ 7 after induction for 72 h.

Optimization of purification process for FMDV VLPs

Traditionally, a sucrose gradient centrifugation has been commonly used for the purification of FMDV VLPs (Vivek Srinivas et al. 2016), which involves complex procedures. To investigate the possibility of affinity chromatography for

FMDV VLPs and simplify the purification method, His₆ tags were added to the N-terminus of VP0, VP3, and VP1, respectively. After the samples were treated with urea, the amount of protein bound to nickel ions increased significantly, and only the VP0, VP3, and VP1 subunit proteins could be detected, indicating that the His₆ tags at the N-terminus of the subunits hindered assembly (Fig. 4b). TEM results showed that when His₆ tags were fused to the N-terminus of these 3 proteins, almost no VLPs could be seen and a large number of pentameric structures were present. When the His₆ tags were removed, assembled VLPs could be detected (Fig. 4c). These results proved that the His₆ tags at the N-terminus of VP0, VP3, and VP1 had a great influence on VLP assembly. Structural analysis of VP0, VP3, and VP1 revealed that residue 136 of VP1 and the C-terminus of VP1 and the C-terminus of VP3 were all located on the surface of the VLPs, while the C-terminus of VP0 was located at the interface of the twofold axis. This region contained a large number of histidines affecting VLPs stability (Fig. 4a). Based on these findings, we further explored the purification process. After induction and cell disruption, the supernatant of GHH, 3 CH, and 1 CH was collected and dialyzed overnight. The eluent was collected after affinity chromatography and detected by WB. The results showed that when detected with anti-His₆ antibodies, only single target bands could be detected (Fig. 4d). When detected with anti-FMDV polyclonal antibodies, three target bands were detected at

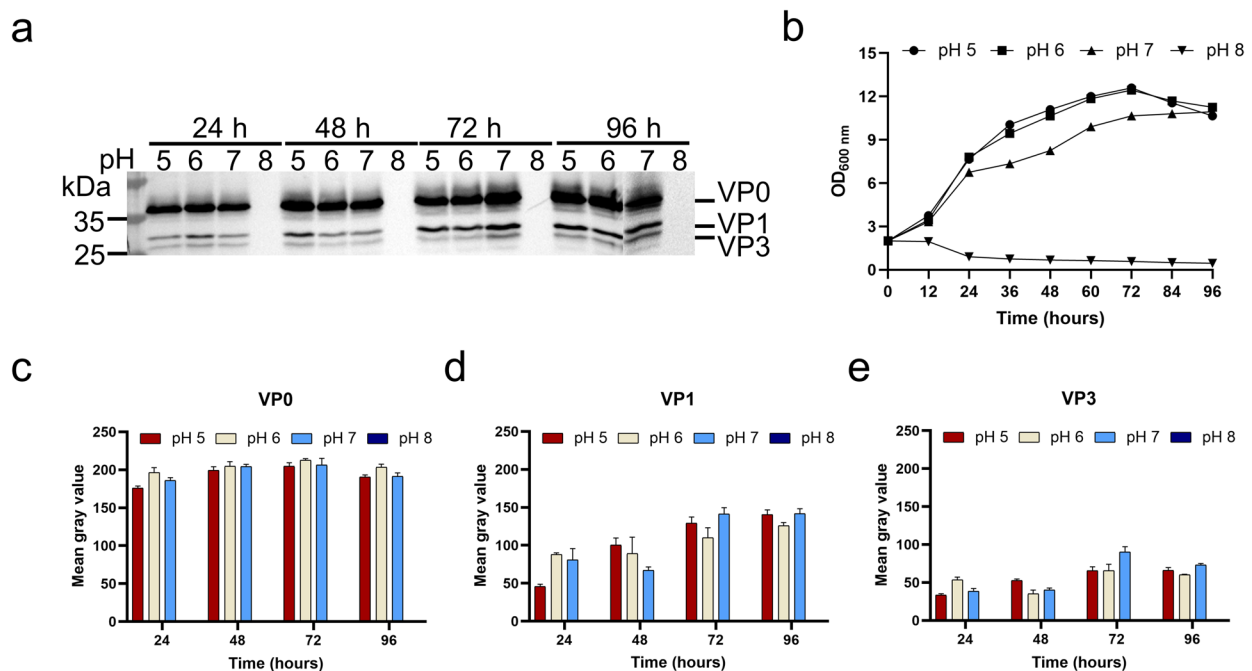
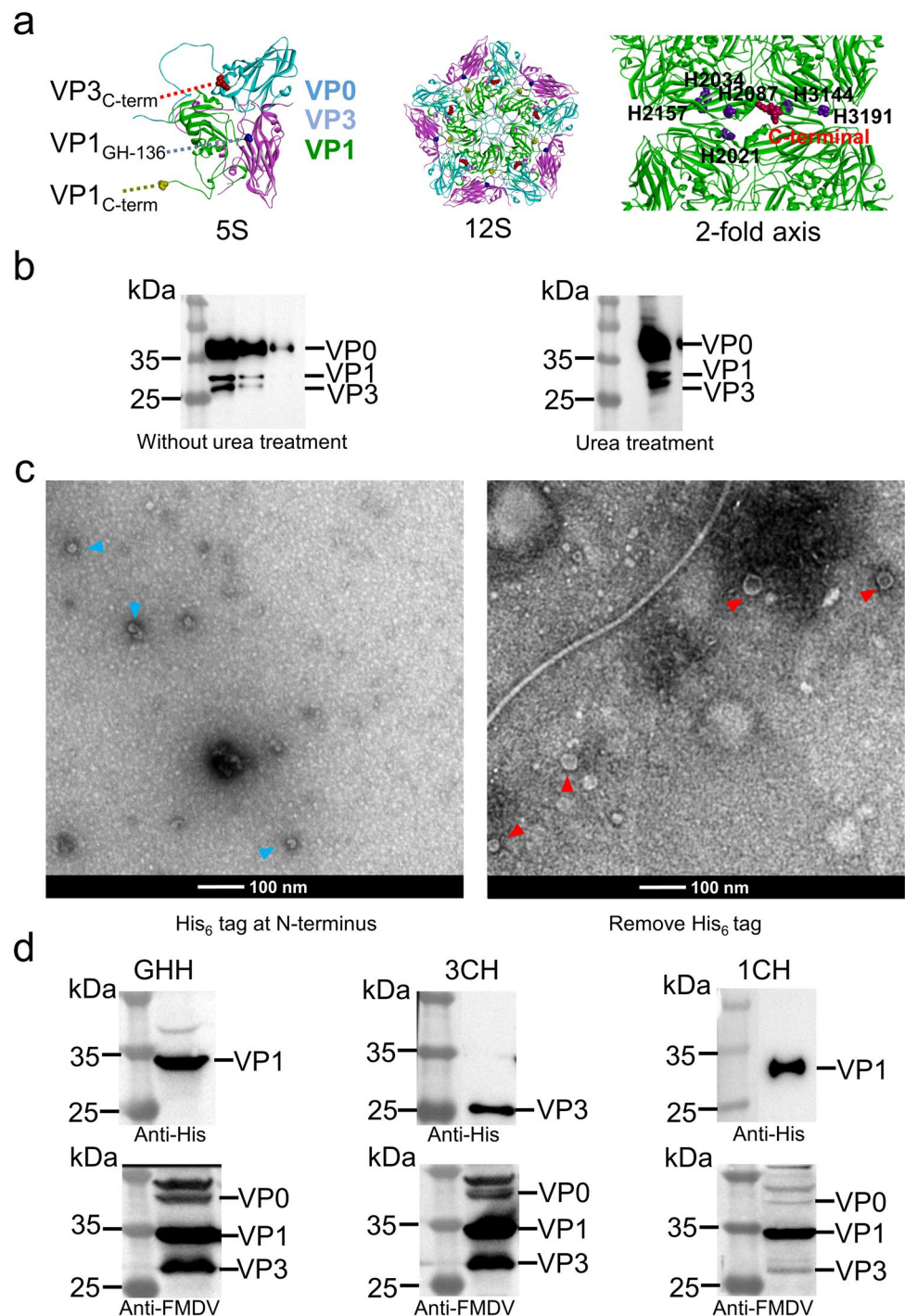


Fig. 3 Optimization of the expression conditions for pPink-130. **a** WB detection of pPink-130 at different time points and pHs. **b** OD values of the pPink-130 strain under different conditions. The expres-

sion levels of VP0 (**c**), VP3 (**d**), and VP1 (**e**) under different conditions were detected by and quantified by Image J (NIH, Bethesda, MD, USA)

Fig. 4 Optimization of the purification for VLPs. **a** Tertiary structure display of the protomers, pentamers, and twofold axis interfaces of FMDV VLPs. VP3_{C-term} means C-terminus of VP3, VP1_{GH-136} means residue 136 of VP1, VP1_{C-term} means C-terminus of VP1, VP0 is shown in magenta, VP3 in cyan, VP1 in green, the C-terminus of VP3 in red, and residue 136 of VP1 in blue. **b** WB detection of the structural proteins of FMDV under conditions with or without urea treatment. **c** TEM of the three subunit proteins with or without the His₆ tags fused to the N-terminus. Pentamers are marked with blue triangles, while VLPs are marked with red triangles. **d** WB detection of GHH, 3CH, and 1CH after affinity chromatography. Scale bar shows 100 nm



25–35 kDa. These results indicate that three subunit proteins with His₆ tags at appropriate positions could be purified simultaneously.

His₆ tags in the G-H region or the C-terminus of VP1 or the C-terminus of VP3 without affecting assembly

To confirm whether the three purified structural proteins could assemble correctly, the samples were detected by TEM

and ELISA. Spherical particles with a diameter of approximately 30 nm could be seen in all samples (Fig. 5a), consistent with the previous TEM images of insect cell-derived VLPs (Porta et al. 2013). Particles were present in GHH, 3CH, and 1CH with average diameters of 31.24 nm, 30.67 nm, and 30.29 nm, respectively (Fig. 5b and c). VLPs in all samples were quantified by measuring the absorbance values using ELISA established in our laboratory. Compared with pPink-130, the VLP antigens per unit volume of GHH and

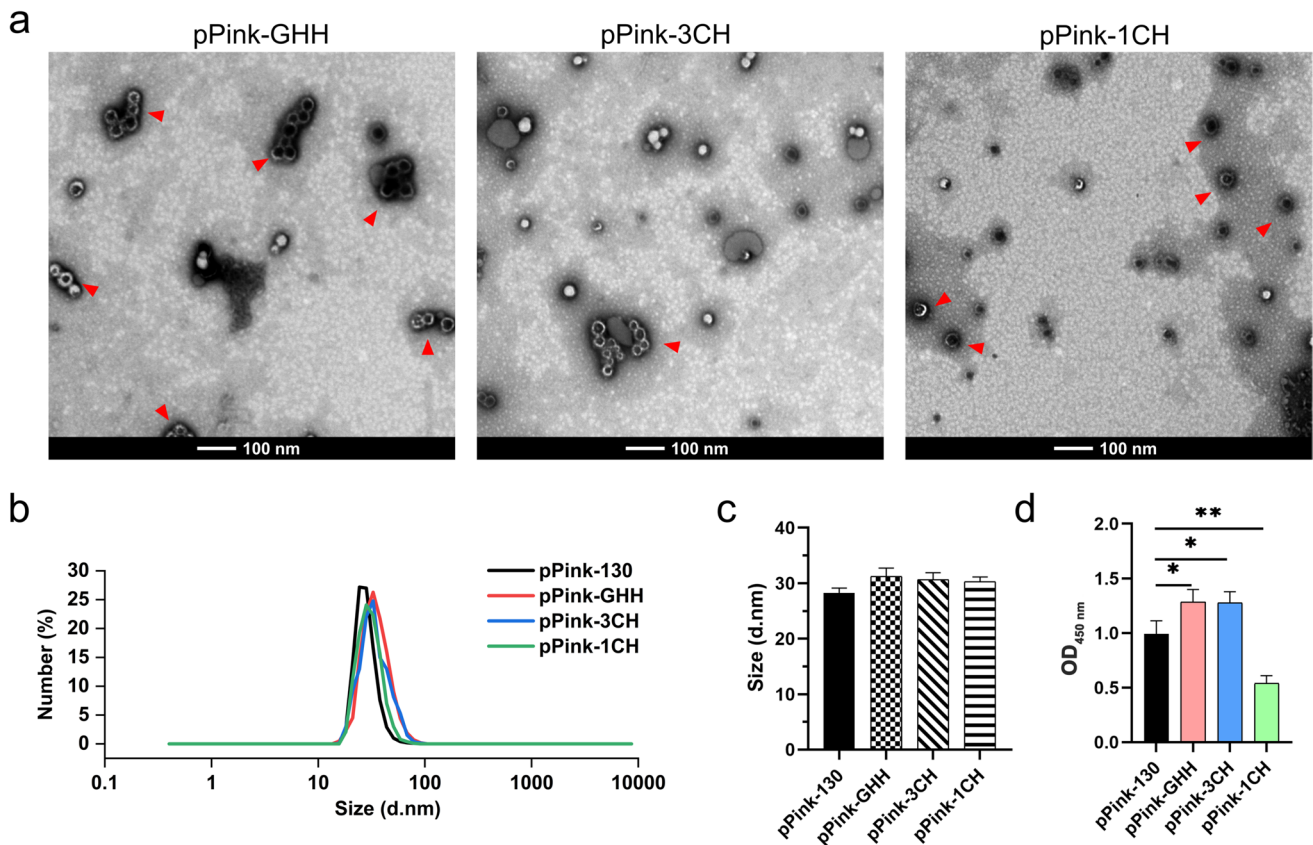


Fig. 5 Assembly of VLPs produced by GHH, 3CH and 1CH. Observation by TEM (a), DLS detection (b), determination of the average particle size (c), and measurement of the VLPs per unit volume (d) of GHH, 3CH, and 1CH after affinity chromatography. “d.nm” represents “diameter in nanometers.” For each construct, the diameters

of particles were measured using Image J ($n = 20$ for particle diameter measurements). Results are presented as means \pm standard deviation. Statistical analysis determined by one-way analysis of variance (ANOVA) (*, $0.01 \leq P < 0.05$, **, $P < 0.01$). Scale bar shows 100 nm

3CH were not lost but slightly increased after affinity chromatography. However, the VLP antigens of 1CH decreased by 50% (Fig. 5d). These findings show that inserting His₆ tags into the C-termini of VP1 or VP3, as well as the G-H region of VP1, does not affect the stability of FMDV VLPs. Leveraging the His₆ affinity tags at these sites, VLPs can be effectively purified by affinity chromatography. Moreover, compared with inserting His₆ tags into the C-terminus of VP1, placing His₆ tags in the G-H region of VP1 or the C-terminus of VP3 enables a significantly higher yield of VLPs.

Discussion

Although some developed countries in Europe and the Americas have eradicated FMD, FMD still causes huge losses to livestock production and economic development in some developing countries, especially low-income countries (Maradei et al. 2013). Currently, inactivated vaccines are the most effective type of vaccine for the prevention and

control of FMD, but they still have some drawbacks in the manufacturing process. VLP vaccines, which have similar immunogenicity to whole virus and do not contain nucleic acids, are the most likely candidates to replace inactivated vaccines (Wang et al. 2016). Although FMD VLPs have been successfully produced in mammalian and baculovirus expression systems, these eukaryotic expression systems also have problems such as high cost and long preparation cycle (Hervas-Stubbs et al. 2007). As we show here, *P. pastoris*, the lowest cost eukaryotic expression system, has been used for the expression of a large number of exogenous proteins (Fernández et al. 2015; Joseph et al. 2016). When co-expressing P1 and 3C of FMDV for the production of VLPs, although a large number of mutations of 3C protease have been carried out in the hope of finding a balance between the cleavage of P1 and the cytotoxicity in the host cell, there is still a problem of cleavage efficiency (Martel et al. 2019; Puckette et al. 2017). Also, the tobacco mosaic virus TEV protease, which was used to replace the FMDV 3C to cleave P1, can produce structural proteins, but no correctly assembled VLPs can be detected (Puckette et al. 2018). The VLPs

of PV, which belongs to the *Picornaviridae* family, have been successfully produced using 2 A instead of 3 C cleavage (Sherry et al. 2023). Here, we investigated the possibility of 3 C protease-independent production of FMDV VLPs in *P. pastoris*.

In this study, the three proteins had different expression preferences in *P. pastoris*. When expressed in their natural order on the P1 protein (VP0-VP3-VP1), the expression level of VP0 was the highest and that of VP1 was the lowest. Interestingly, after adjusting the order of the expression cassettes of VP0 and VP1, the difference in their expression was reduced. It has been speculated that the repeated promoters on the plasmid might compete for RNA polymerase, leading to the phenomenon of “transcriptional attenuation,” which has also been observed in the production of multi-subunit VLPs in *P. pastoris* (Rodríguez-Limas et al. 2011; Saraswat et al. 2016). Notably, the expression level of the VP0 protein was always the highest in *P. pastoris*, regardless of whether it was located upstream or downstream of the plasmid. Interestingly, VLPs could be detected in both pPink-031 and pPink-130 after sucrose gradient centrifugation. However, it was found that although a large amount of VP0 protein could be co-sedimented in pPink-031, the yield of VLPs was very low. In contrast, more VLPs were detected in pPink-130, where the expression levels of VP0, VP3, and VP1 were more optimized, as also observed by TEM (Fig. 2).

In general, pH and induction time have a significant influence on the expression of exogenous proteins in *P. pastoris*. Yeast cells can grow at pH values ranging from 3 to 7. However, to maintain metabolic activities and reduce degradation of exogenous proteins within the yeast cells, pH is usually controlled between 5 and 6 (Cregg et al. 1993). Of all the picornaviruses, FMDV is the most sensitive to acidic pH and the virions dissociate into pentamers under slightly acidic conditions (Curry et al. 1995). The N1017D and H2145Y mutations in FMDV are the most acid-resistant, and after undergoing the N1017D and H2145Y mutations, the virus still retains relatively high infectivity at pH 5.4 (Caridi et al. 2020; Vázquez-Calvo et al. 2014). Therefore, to find the optimal culture pH conditions for FMDV VLP production in *P. pastoris* during shake flask cultivation, the pPink-130 strain was induced to express structural proteins at different pHs. It was found that both yeast cell growth and protein expression were severely affected. However, notably, although the yeast OD value decreased, a relatively high level of protein expression was achieved. These results suggest that a balance has been struck between yeast cell growth and expression of FMDV structural proteins. Moreover, determining the optimum induction time can save both raw material and time costs.

Currently, chemical separation and sucrose gradient purification are commonly used. These methods require

high-specification centrifuges and are only suitable for small batches production. To find a suitable purification method for industrial production, the feasibility of purifying VLPs by affinity chromatography was investigated. It is known that the N-termini of the VP0, VP3, and VP1 proteins are located inside the VLPs, the C-terminus of VP0 is located at the 2-axis fold interface, and the protonation of histidines in this region at acidic pH is the main cause of VLP instability, while the C-termini of VP3 and VP1 are located on the surface of the VLPs (Acharya et al. 1989; Curry et al. 1997; van Vlijmen et al. 1998), which is consistent with our results (Fig. 4). Inserting the flag tags into the G-H loop region of VP1 does not affect the assembly of VLPs, and it can be displayed on the surface (Lawrence et al. 2013). Therefore, three positions were finally chosen for the insertion of the His₆ tags. The results showed that, after affinity chromatography, the three structural proteins can be captured simultaneously by these single His₆ tags. FMDV VLPs can be assembled by non-covalent binding of subunit proteins, allowing affinity purification of VLPs that are morphologically similar to the natural virus. The ELISA results show that the amount of VLPs in 3 CH per unit volume did not decrease significantly after affinity chromatography compared to pPink-130. Previously, it has been reported that fusing a short peptide at the C-terminus of VP3 of poliovirus, which belongs to the *Picornaviridae* family, did not affect the assembly and antigenicity of VLPs (Sherry et al. 2023). In our study, VLPs in 3 CH could also be successfully purified after affinity chromatography. Similarly, although the amount of VLPs in 1 CH are not high per unit volume, the addition of short peptides inserted at the C-terminus of VP1 does not affect the assembly of VLPs, consistent with previous reports (Gullberg et al. 2013; Kristensen et al. 2017). We also observed the apparent differences in the proportions of the structural proteins detected in GHH, 3 CH, and 1 CH. This may be attributed to several factors. Firstly, regarding the different samples (GHH, 3 CH, and 1 CH), the genetic constructs and the way the His₆ tag is fused may affect the expression and stability of the proteins. Moreover, the affinity chromatography process itself could also contribute to these differences. The binding affinity of the His₆ tagged proteins to the chromatography resin might vary depending on the local environment of the His₆ tag within the protein structure. Proteins with different conformations or steric hindrances around the His₆ tag may bind to the resin with different efficiencies, leading to differential elution profiles and thus different proportions of proteins detected in the WB.

In summary, VLPs were successfully produced in *P. pastoris* similar to those generated from mammalian cells using a 3 C protease-independent approach. In addition, structural analysis of FMDV VLPs revealed that His₆ tags can be attached to the G-H loop and C-terminus of VP1 and the C-terminus of VP3 without affecting the assembly

and immunogenicity, laying the foundation for the purification and industrial production of VLPs. In conclusion, the protease-independent system provides a reference for the development of FMDV VLP vaccines and offers insights into the production of other picornavirus virus-like particles or the purification and assembly of multi-subunit VLPs.

Supplementary Information The online version contains supplementary material available at <https://doi.org/10.1007/s00253-025-13510-5>.

Acknowledgements We are deeply indebted to our research team members, Zhidong Teng, Lingbo Chen, and Jin Wang, for their assistance in conducting experiments and their valuable suggestions during the research process.

Author contribution HCG, ZYL, and SQS: conceptualization and designing. ZYL: conducted the experiments and wrote the manuscript. HD: methodology and revised the manuscript. SHY, MYB, YZ, and YZD: collected and analyzed data. HCG and SQS: project administration, supervision and review.

Funding This study was partly funded by the Technology Innovation Guidance Program of Gansu Province (24 CXNA030), Key R&D Program of Ningxia Province (2024BBF02017), Lanzhou Talent Innovation and Entrepreneurship Project (2023-RC-3), the Major Science and Technology Project of Gansu Province (24ZDWA004), and China Postdoctoral Science Foundation Funded Project (2023M733819, 2024M763620).

Data availability All the data supporting the findings of this study are available within the paper.

Declarations

Ethics approval This study did not involve any animal experiments, and thus no ethics approval specific to animal research was required.

Conflict of interest The authors declare no competing interests.

Open Access This article is licensed under a Creative Commons Attribution-NonCommercial-NoDerivatives 4.0 International License, which permits any non-commercial use, sharing, distribution and reproduction in any medium or format, as long as you give appropriate credit to the original author(s) and the source, provide a link to the Creative Commons licence, and indicate if you modified the licensed material. You do not have permission under this licence to share adapted material derived from this article or parts of it. The images or other third party material in this article are included in the article's Creative Commons licence, unless indicated otherwise in a credit line to the material. If material is not included in the article's Creative Commons licence and your intended use is not permitted by statutory regulation or exceeds the permitted use, you will need to obtain permission directly from the copyright holder. To view a copy of this licence, visit <http://creativecommons.org/licenses/by-nc-nd/4.0/>.

References

- Acharya R, Fry E, Stuart D, Fox G, Rowlands D, Brown F (1989) The three-dimensional structure of foot-and-mouth disease virus at 2.9 Å resolution. *Nature* 337(6209):709–716. <https://doi.org/10.1038/337709a0>
- Alexandersen S, Zhang Z, Donaldson AI, Garland AJ (2003) The pathogenesis and diagnosis of foot-and-mouth disease. *J Comp Pathol* 129(1):1–36. [https://doi.org/10.1016/s0021-9975\(03\)00041-0](https://doi.org/10.1016/s0021-9975(03)00041-0)
- Arzt J, Juleff N, Zhang Z, Rodriguez LL (2011) The pathogenesis of foot-and-mouth disease I: viral pathways in cattle. *Transbound Emerg Dis* 58(4):291–304. <https://doi.org/10.1111/j.1865-1682.2011.01204.x>
- Belsham GJ, McInerney GM, Ross-Smith N (2000) Foot-and-mouth disease virus 3C protease induces cleavage of translation initiation factors eIF4A and eIF4G within infected cells. *J Virol* 74(1):272–280. <https://doi.org/10.1128/jvi.74.1.272-280.2000>
- Capozzo AV, Burke DJ, Fox JW, Bergmann IE, La Torre JL, Grigera PR (2002) Expression of foot and mouth disease virus non-structural polypeptide 3ABC induces histone H3 cleavage in BHK21 cells. *Virus Res* 90(1–2):91–99. [https://doi.org/10.1016/s0168-1702\(02\)00140-5](https://doi.org/10.1016/s0168-1702(02)00140-5)
- Cardi F, López-Argüello S, Rodríguez-Huete A, Torres E, Bustos MJ, Cañas-Arranz R, Martín-Acebes MA, Mateu MG, Sobrino F (2020) Negatively charged amino acids at the foot-and-mouth disease virus capsid reduce the virion-destabilizing effect of viral RNA at acidic pH. *Sci Rep* 10(1):1657. <https://doi.org/10.1038/s41598-020-58414-8>
- Chackerian B (2007) Virus-like particles: flexible platforms for vaccine development. *Expert Rev Vaccines* 6(3):381–390. <https://doi.org/10.1586/14760584.6.3.381>
- Cregg JM, Vedvick TS, Raschke WC (1993) Recent advances in the expression of foreign genes in *Pichia pastoris*. *Biotechnology (NY)* 11(8):905–910. <https://doi.org/10.1038/nbt0893-905>
- Curry S, Abrams CC, Fry E, Crowther JC, Belsham GJ, Stuart DI, King AM (1995) Viral RNA modulates the acid sensitivity of foot-and-mouth disease virus capsids. *J Virol* 69(1):430–438. <https://doi.org/10.1128/jvi.69.1.430-438.1995>
- Curry S, Fry E, Blakemore W, Abu-Ghazaleh R, Jackson T, King A, Lea S, Newman J, Stuart D (1997) Dissecting the roles of VP0 cleavage and RNA packaging in picornavirus capsid stabilization: the structure of empty capsids of foot-and-mouth disease virus. *J Virol* 71(12):9743–9752. <https://doi.org/10.1128/jvi.71.12.9743-9752.1997>
- de Felipe P, Luke GA, Hughes LE, Gani D, Halpin C, Ryan MD (2006) E unum pluribus: multiple proteins from a self-processing polypeptide. *Trends Biotechnol* 24(2):68–75. <https://doi.org/10.1016/j.tibtech.2005.12.006>
- Dong H, Liu P, Bai M, Wang K, Feng R, Zhu D, Sun Y, Mu S, Li H, Harmsen M, Sun S, Wang X, Guo H (2022) Structural and molecular basis for foot-and-mouth disease virus neutralization by two potent protective antibodies. *Protein Cell* 13(6):446–453. <https://doi.org/10.1007/s13238-021-00828-9>
- Feng Q, He Y, Lu J (2016) Virus-like particles produced in *Pichia pastoris* induce protective immune responses against coxsackievirus A16 in mice. *Med Sci Monit* 22:3370–3382. <https://doi.org/10.12659/msm.900380>
- Fernández E, Toledo JR, Mansur M, Sánchez O, Gil DF, González-González Y, Lamazares E, Fernández Y, Parra F, Farnós O (2015) Secretion and assembly of calicivirus-like particles in high-cell-density yeast fermentations: strategies based on a recombinant non-specific BPTI-Kunitz-type protease inhibitor. *Appl Microbiol Biotechnol* 99(9):3875–3886. <https://doi.org/10.1007/s00253-014-6171-z>
- Gullberg M, Polacek C, Bötner A, Belsham GJ (2013) Processing of the VP1/2A junction is not necessary for production of foot-and-mouth disease virus empty capsids and infectious viruses: characterization of “self-tagged” particles. *J Virol* 87(21):11591–11603. <https://doi.org/10.1128/jvi.01863-13>
- Hervas-Stubbs S, Rueda P, Lopez L, Leclerc C (2007) Insect baculoviruses strongly potentiate adaptive immune responses by inducing

- type I IFN. *J Immunol* 178(4):2361–2369. <https://doi.org/10.4049/jimmunol.178.4.2361>
- Joseph NM, Ho KL, Tey BT, Tan CS, Shafee N, Tan WS (2016) Production of the virus-like particles of nipah virus matrix protein in *Pichia pastoris* as diagnostic reagents. *Biotechnol Prog* 32(4):1038–1045. <https://doi.org/10.1002/btpr.2279>
- Kim JH, Lee SR, Li LH, Park HJ, Park JH, Lee KY, Kim MK, Shin BA, Choi SY (2011) High cleavage efficiency of a 2A peptide derived from porcine teschovirus-1 in human cell lines, zebrafish and mice. *PLoS ONE* 6(4):e18556. <https://doi.org/10.1371/journal.pone.0018556>
- Kristensen T, Normann P, Gullberg M, Fahnøe U, Polacek C, Rasmussen TB, Belsham GJ (2017) Determinants of the VP1/2A junction cleavage by the 3C protease in foot-and-mouth disease virus-infected cells. *J Gen Virol* 98(3):385–395. <https://doi.org/10.1099/jgv.0.000664>
- Lawrence P, Pacheco JM, Uddowla S, Hollister J, Kotecha A, Fry E, Rieder E (2013) Foot-and-mouth disease virus (FMDV) with a stable FLAG epitope in the VP1 G-H loop as a new tool for studying FMDV pathogenesis. *Virology* 436(1):150–161. <https://doi.org/10.1016/j.virol.2012.11.001>
- Li Z, Ma Y, Nan X, Dong H, Tang J, Yin S, Sun S, Bao E, Guo H (2024) Production of virus-like particles of FMDV by 3C protease cleaving precursor polypeptide P1 in vitro. *Appl Microbiol Biotechnol* 108(1):542. <https://doi.org/10.1007/s00253-024-13376-z>
- Maradei E, Malirat V, Beascoechea CP, Benitez EO, Pedemonte A, Seki C, Novo SG, Balette CI, D'Aloia R, La Torre JL, Mattion N, Toledo JR, Bergmann IE (2013) Characterization of a type O foot-and-mouth disease virus re-emerging in the year 2011 in free areas of the Southern Cone of South America and cross-protection studies with the vaccine strain in use in the region. *Vet Microbiol* 162(2–4):479–490. <https://doi.org/10.1016/j.vetmic.2012.10.035>
- Martel E, Forzono E, Kurker R, Clark BA, Neilan JG, Puckette M (2019) Effect of foot-and-mouth disease virus 3C protease B2 β -strand proline mutagenesis on expression and processing of the P1 polypeptide using a plasmid expression vector. *J Gen Virol* 100(3):446–456. <https://doi.org/10.1099/jgv.0.001204>
- McAleer WJ, Buynak EB, Maigetter RZ, Wampler DE, Miller WJ, Hilleman MR (1984) Human hepatitis B vaccine from recombinant yeast. *Nature* 307(5947):178–180. <https://doi.org/10.1038/307178a0>
- Mignaquí AC, Ruiz V, Perret S, St-Laurent G, Singh Chahal P, Transfiguración J, Sammarruco A, Gnazzo V, Durocher Y, Wigdorovitz A (2013) Transient gene expression in serum-free suspension-growing mammalian cells for the production of foot-and-mouth disease virus empty capsids. *PLoS ONE* 8(8):e72800. <https://doi.org/10.1371/journal.pone.0072800>
- Mignaquí AC, Ruiz V, Durocher Y, Wigdorovitz A (2019) Advances in novel vaccines for foot and mouth disease: focus on recombinant empty capsids. *Crit Rev Biotechnol* 39(3):306–320. <https://doi.org/10.1080/07388551.2018.1554619>
- Mignaquí AC, Ferella A, Cass B, Mukankurayija L, L'Abbé D, Bisson L, Sánchez C, Scian R, Cardillo SB, Durocher Y, Wigdorovitz A (2020) Foot-and-mouth disease: optimization, reproducibility, and scalability of high-yield production of virus-like particles for a next-generation vaccine. *Front Vet Sci* 7:601. <https://doi.org/10.3389/fvets.2020.00601>
- Polacek C, Gullberg M, Li J, Belsham GJ (2013) Low levels of foot-and-mouth disease virus 3C protease expression are required to achieve optimal capsid protein expression and processing in mammalian cells. *J Gen Virol* 94(6):1249–1258. <https://doi.org/10.1099/vir.0.050492-0>
- Porta C, Xu X, Loureiro S, Paramasivam S, Ren J, Al-Khalil T, Burman A, Jackson T, Belsham GJ, Curry S, Lomonosoff GP, Parida S, Paton D, Li Y, Wilsden G, Ferris N, Owens R, Kotecha A, Fry E, Stuart DI, Charleston B, Jones IM (2013) Efficient production of foot-and-mouth disease virus empty capsids in insect cells following down regulation of 3C protease activity. *J Virol Methods* 187(2):406–412. <https://doi.org/10.1016/j.jviro.2012.11.011>
- Puckette M, Clark BA, Smith JD, Turecek T, Martel E, Gabbert L, Pisano M, Hurtle W, Pacheco JM, Barrera J, Neilan JG, Rasmussen M (2017) Foot-and-mouth disease (FMD) virus 3C protease mutant L127P: implications for FMD vaccine development. *J Virol* 91(22):e00924. <https://doi.org/10.1128/jvi.00924-17>
- Puckette M, Smith JD, Gabbert L, Schutta C, Barrera J, Clark BA, Neilan JG, Rasmussen M (2018) Production of foot-and-mouth disease virus capsid proteins by the TEV protease. *J Biotechnol* 275:7–12. <https://doi.org/10.1016/j.jbiotec.2018.03.012>
- Robinson L, Knight-Jones TJ, Charleston B, Rodriguez LL, Gay CG, Sumption KJ, Vosloo W (2016) Global foot-and-mouth disease research update and gap analysis: 3-vaccines. *Transbound Emerg Dis* 63(Suppl 1):30–41. <https://doi.org/10.1111/tbed.12521>
- Rodríguez-Limas WA, Tyo KE, Nielsen J, Ramírez OT, Palomares LA (2011) Molecular and process design for rotavirus-like particle production in *Saccharomyces cerevisiae*. *Microb Cell Fact* 10:33. <https://doi.org/10.1186/1475-2859-10-33>
- Saraswat S, Athmaram TN, Parida M, Agarwal A, Saha A, Dash PK (2016) Expression and characterization of yeast derived chikungunya virus like particles (CHIK-VLPs) and its evaluation as a potential vaccine candidate. *PLoS Negl Trop Dis* 10(7):e0004782. <https://doi.org/10.1371/journal.pntd.0004782>
- Sasagawa T, Pushko P, Steers G, Gschmeissner SE, Hajibagheri MA, Finch J, Crawford L, Tommasino M (1995) Synthesis and assembly of virus-like particles of human papillomaviruses type 6 and type 16 in fission yeast *Schizosaccharomyces pombe*. *Virology* 206(1):126–135. [https://doi.org/10.1016/s0042-6822\(95\)80027-1](https://doi.org/10.1016/s0042-6822(95)80027-1)
- Sherry L, Grehan K, Snowden JS, Knight ML, Adeyemi OO, Rowlands DJ, Stonehouse NJ (2020) Comparative molecular biology approaches for the production of poliovirus virus-like particles using *Pichia pastoris*. *mSphere* 5(2):e00838. <https://doi.org/10.1128/mSphere.00838-19>
- Sherry L, Swanson JJ, Grehan K, Xu H, Uchida M, Jones IM, Stonehouse NJ, Rowlands DJ (2023) Protease-independent production of poliovirus virus-like particles in *Pichia pastoris*: implications for efficient vaccine development and insights into capsid assembly. *Microbiol Spectr* 11(1):e0430022. <https://doi.org/10.1128/spectrum.04300-22>
- Smith J, Lipsitch M, Almond JW (2011) Vaccine production, distribution, access, and uptake. *Lancet* 378(9789):428–438. [https://doi.org/10.1016/s0140-6736\(11\)60478-9](https://doi.org/10.1016/s0140-6736(11)60478-9)
- Subramaniam S, Sanyal A, Mohapatra JK, Sharma GK, Biswal JK, Ranjan R, Rout M, Das B, Bisht P, Mathapati BS, Dash BB, Pattnaik B (2013) Emergence of a novel lineage genetically divergent from the predominant Ind 2001 lineage of serotype O foot-and-mouth disease virus in India. *Infect Genet Evol* 18:1–7. <https://doi.org/10.1016/j.meegid.2013.04.027>
- van Vlijmen HW, Curry S, Schaefer M, Karplus M (1998) Titration calculations of foot-and-mouth disease virus capsids and their stabilities as a function of pH. *J Mol Biol* 275(2):295–308. <https://doi.org/10.1006/jmbi.1997.1418>
- Vázquez-Calvo A, Caridi F, Sobrino F, Martín-Acebes MA (2014) An increase in acid resistance of foot-and-mouth disease virus capsid is mediated by a tyrosine replacement of the VP2 histidine previously associated with VP0 cleavage. *J Virol* 88(5):3039–3042. <https://doi.org/10.1128/jvi.03222-13>
- Veerapen VP, van Zyl AR, Wigdorovitz A, Rybicki EP, Meyers AE (2018) Novel expression of immunogenic foot-and-mouth disease virus-like particles in *Nicotiana benthamiana*. *Virus Res* 244:213–217. <https://doi.org/10.1016/j.virusres.2017.11.027>
- Vivek Srinivas VM, Basagoudanavar SH, Hosamani M (2016) IRES mediated expression of viral 3C protease for enhancing the yield

- of FMDV empty capsids using baculovirus system. *Biologicals* 44(2):64–68. <https://doi.org/10.1016/j.biologicals.2015.12.002>
- Wang M, Jiang S, Wang Y (2016) Recent advances in the production of recombinant subunit vaccines in *Pichia pastoris*. *Bioengineered* 7(3):155–165. <https://doi.org/10.1080/21655979.2016.1191707>
- Xie Y, Li H, Qi X, Ma Y, Yang B, Zhang S, Chang H, Yin X, Li Z (2019) Immunogenicity and protective efficacy of a novel foot-and-mouth disease virus empty-capsid-like particle with improved acid stability. *Vaccine* 37(14):2016–2025. <https://doi.org/10.1016/j.vaccine.2019.02.032>
- Zhang C, Ku Z, Liu Q, Wang X, Chen T, Ye X, Li D, Jin X, Huang Z (2015) High-yield production of recombinant virus-like particles of enterovirus 71 in *Pichia pastoris* and their protective efficacy against oral viral challenge in mice. *Vaccine* 33(20):2335–2341. <https://doi.org/10.1016/j.vaccine.2015.03.034>

Publisher's Note Springer Nature remains neutral with regard to jurisdictional claims in published maps and institutional affiliations.